Green process for green materials: viable low temperature lipase-catalysed synthesis of renewable telechelics in supercritical CO_2

S. Curia[a], A.F. Barclay[a], S. Torron[b], M. Johansson[b], S.M. Howdle[a]*

[a]:*University of Nottingham, School of Chemistry, University Park, Nottingham, NG7 2RD, UK*
[b]: *Department of Fibre and Polymer Technology, KTH Royal Institute of Technology, Stockholm, Sweden*
Keywords: azelaic acid, supercritical CO_2, lipase, telechelics.

Summary

We present a novel near ambient temperature approach to telechelic renewable polyesters by exploiting the unique properties of supercritical CO_2 ($scCO_2$). Bio-based commercially available monomers have been polymerised and functional telechelic materials with targeted molecular weight were prepared by end-capping the chains with molecules containing reactive moieties in a one-pot reaction. The use of $scCO_2$ as a reaction medium facilitates the effective use of Candida Antarctica Lipase B (CaLB) as a catalyst at a temperature as low as 35 °C, hence avoiding side reactions, maintaining the end-capper functionality and preserving the enzyme activity.
The functionalised polymer products have been characterised by ^{1}H-NMR, MALDI-TOF, GPC and DSC in order to carefully assess their structural and thermal properties.
We demonstrate that telechelic materials can be produced enzymatically at mild temperatures, in a solvent-free system and using renewably sourced monomers without pre-modification, by exploiting the unique properties of $scCO_2$. The macromolecules we prepare are ideal green precursors that can be further reacted to prepare useful bio-derived films and coatings.

Main Text

1. Introduction

The use of green monomers to replace non-renewable and fossil-based raw materials is an important research focus of modern polymer science, both in academia and industry (1-4). Biodegradable and renewable plastics are being developed to limit the use of plastics derived from petroleum that at the end of their life cycle are usually incinerated or disposed of in landfills, thus representing a serious environmental issue (5).
Applications of green plastics range from food packaging (6), medical and tissue engineering (7), through to fabrics and coatings (4), to name just a few. Recently, great importance has been given to low molecular weight (between 1000 and 4000 g/mol) telechelic polyesters (8-11). These are functional polymers that carry the same functional group at both ends (12) and find applications in surface modification (8, 9), medical materials (13), block copolymer formation (14), cross-linked networks (10, 15) *etc*.
Low molecular weights are often desirable in order to obtain low-viscosity materials and good filmability (8, 10, 11). Furthermore, if a cross-linkable system is the desired product, low molecular weight between the reactive moieties is necessary in order to achieve a high cross-link density and therefore a tougher network (8, 10, 15).
To achieve a fully green process, enzymes have been exploited as substitutes for metal-based catalysts that are potentially toxic (16-19), expensive, and require high temperatures (normally greater than 160 °C for polycondensations) to work effectively (20-24). By employing enzymes, polymeric materials have been synthesised through ring-opening and condensation polymerisations (9, 25, 26). Furthermore, the specificity of enzymes allows for preservation of particular functional groups, which can be exploited subsequently for further

*Author for correspondence (Steve.Howdle@Nottingham.ac.uk).
University of Nottingham, School of Chemistry, University Park
Nottingham, NG7 2RD, UK

reaction processing (19). One key drawback is that at higher temperatures side reactions involving other chemical groups do occur, thus leading to branching and cross-linking (26, 27). Furthermore, at temperatures higher than 100 °C the activity of CaLB is vastly reduced (28), hence making high-temperature processes not commercially sustainable.
Enzymatic poly-condensations are normally carried out in apolar solvents (*e.g.* toluene) or in the bulk (10, 19, 26). Unfortunately, owing to the high melting point (>100 °C) of most natural occurring diacids, the melt processes are limited. Moreover, the diacids usually are not soluble in apolar media, and aprotic solvents (*e.g.* methanol) cannot be used because they would prevent effective polycondensation. The work-around is to introduce an extra step, to esterify the diacids and to work from the diesters (9, 29-31). Unfortunately, this is not always desirable and extra steps can impact dramatically upon the viability of a commercial process.
In recent years interest in the use of compressed CO_2 as a reaction medium or plasticiser for polymer synthesis and processing has increased steeply (32-35). CO_2 has been exploited as a solvent for polymerisations (36, 37), as a foaming agent (32, 38), for precipitation/separation (39), particle formation (40, 41) and encapsulation (42).
High-pressure CO_2 is a good solvent for many small molecules and it is very effective at plasticising and effectively liquefying many polymers at temperatures below their glass transition temperature (T_g) and melting point (T_m) (33, 41, 43-52), therefore opening up new opportunities for polymer synthesis and modification.
In this paper we demonstrate the synthesis of novel green telechelics through near-room-temperature (35 °C) enzymatic poly-condensations of azelaic acid and 1,6-hexanediol in $scCO_2$.
Azelaic acid is an naturally occurring saturated dicarboxylic acid with T_m ~110 °C (**Figure 1**), slightly soluble in $scCO_2$ (53), which is found in wheat, rye and barley (54). It can also be produced through ozonolysis of oleic acid (53, 55). This diacid is not soluble in apolar solvents and the only polymerisations shown in literature were performed in the bulk with the aid of metal catalysts at temperatures as high as 230 °C (56, 57) which are required to melt the diacid and activate the catalyst.

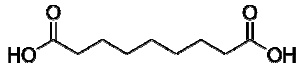

Figure 1 – Azelaic acid is a naturally occurring diacid with T_m ~110 °C.

In our near-room temperature enzymatic polycondensations, the molecular weight of the chains was targeted by using functional end-cappers. Namely, sorbic alcohol (SA), 12-hydroxy stearic acid (HSA), 2-hydroxyethyl methacrylate (HEMA) and trimethylolpropane oxetane (TMPO) were used (**Figure 2**).
These molecules contain one moiety able to undergo condensation and another one useful for further reaction (*e.g.* cross-linking or chain extension). In more detail, SA is a diene that can undergo Diels-Alder addition and thiol-ene click chemistry, HSA contains a secondary hydroxyl group that can be cross-linked with isocyanates, HEMA is characterised by a double bond that can be radically reacted, finally TMPO is an oxetane derivative that can be ring-opened by using a Lewis acid.
Furthermore, SA is a naturally occurring molecule and HSA is produced through hydrogenation of castor oil; hence, the bio-content of the polymers obtained with these two functionalisers is 100%.

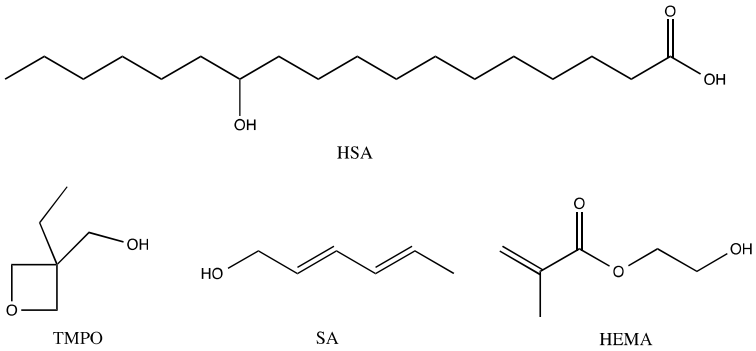

Figure 2 - The functional end-cappers used in this study.

We hypothesised that combined use of CaLB and $scCO_2$, and consequent mild temperature, would ensure minimal side reactions, thus preserving the end-cappers functionality. Furthermore, our aim is to show that the enzyme can be re-used without loss of activity.
Therefore, in this paper we show that thanks to $scCO_2$ it is possible to prepare a range of green functional materials with targeted degree of polymerisation (DP) through enzymatic syntheses at near-room-temperature conditions and without pre-modification of the monomers. This route could be particularly valuable for all those applications where the incorporation of thermally labile functional groups or additives (*e.g.* proteins, drugs,

hormones *etc.*) is desired. Thus, our aim is to exploit the unique properties of $scCO_2$ to prepare green functional materials through a novel low-temperature approach.

2. Experimental

2.1 Materials

All chemicals and solvents were purchased from Sigma Aldrich (UK), unless otherwise indicated. Novozym 435 (CaLB immobilised on cross-linked acrylic resin beads) was kindly donated by Novozymes (Denmark) stored at 4 °C and dried for 24 h under vacuum (100 mbar) at room temperature (RT) before use. Azelaic acid was purchased from Alfa Aesar (UK) and dried for 24 h under vacuum (100 mbar) at 50 °C before use. The other reagents were dried at RT for 24 h under vacuum (100 mbar) before use. All the solvents were of analytical grade, or Chromasolv® were specified, and used as received. Supercritical Fluid Chromatography (SFC) grade 4.0 CO_2 (minimum purity 99.99%) was purchased from BOC Special Gases (UK) and used as received.

2.2 Methods

Enzymatic synthesis of telechelic poly(hexylene azelate) (PHA). In a typical procedure the diacid (10.20 mmol), diol (7.65 mmol) and one end-capper chosen from SA, HEMA and TMPO (5.10 mmol) were added to the stainless steel reaction autoclave (60 mL) (35, 37), along with enzyme and fresh molecular sieves (3 Å, particle size 1.6-2.5 nm) (25% by weight of each relative to the total amount of monomers and end-cappers). The vessel was then sealed and pressurised up to 50 bar. The temperature was then raised to 35 °C, the pressure stabilised at 275 bar and the reaction left to run for 24 h while stirring at 100 rpm. To avoid polymer foaming and consequent tubing blockages (25), the reactions were stopped by cooling the vessel in a water/ice bath (0 °C) and the CO_2 was vented when the pressure went below 20 bar. Finally, the product was dissolved in 6 mL of toluene and filtered to remove the enzyme and sieves. Filtered solutions were dried at 40 °C under reduced pressure leaving solid polymeric products. Product yield was calculated dividing the dry product mass by the theoretical mass.
When using HSA as an end-capper, an excess of diol was used in order to obtain –OH functional chains able to react with the hydroxy fatty acid. Therefore, 10.20 mmol of diol and 7.65 mmol (DP3) of diacid were used. The reaction conditions and purification procedure were as described above.
The reactions were performed at least twice to check reproducibility. The naming scheme used in this paper is detailed in **Table 1**.

Table 1 – Naming scheme of the telechelic poly(hexylene azelate)s (PHAs) presented in this paper

Name	Functionaliser
PHA-SA	Sorbic alcohol (SA)
PHA-HSA	12-hydroxy stearic acid (HSA)
PHA-TMPO	Trimethylolpropane oxetane (TMPO)
PHA-HEMA	2-hydroxyethyl methacrylate (HEMA)

The reaction schemes are shown below (**Figure 3**).

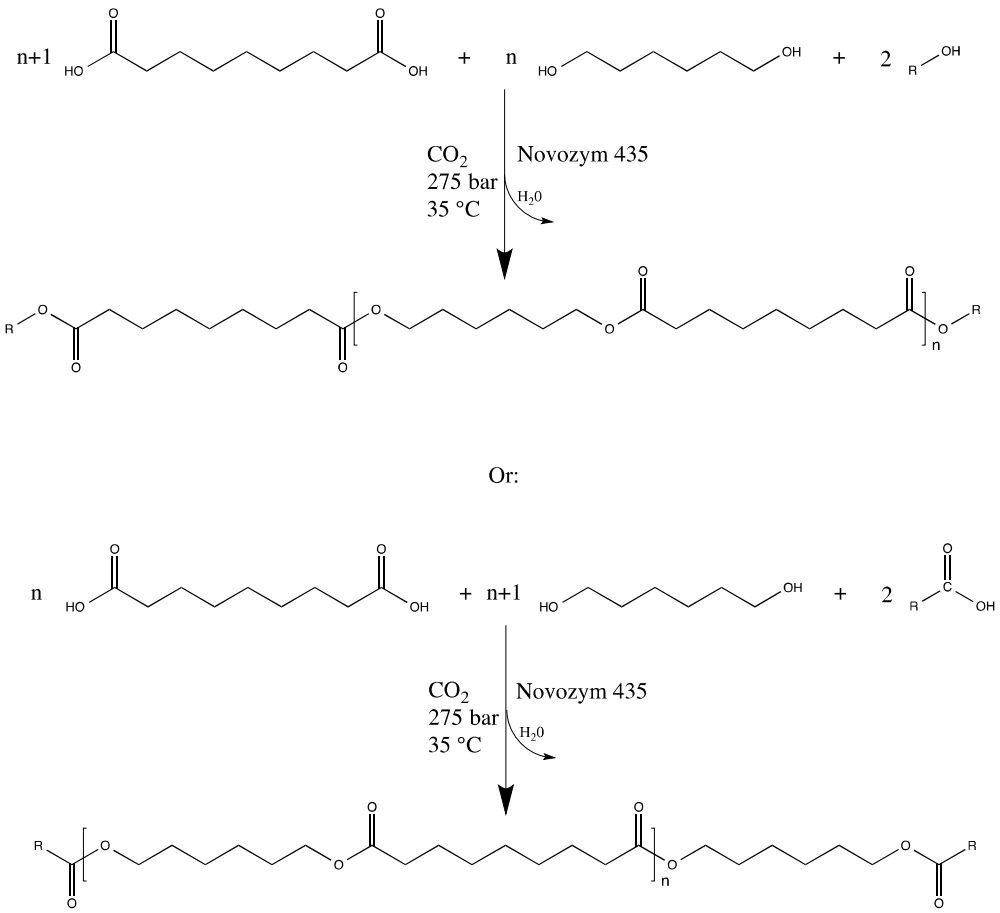

Figure 3 – Reaction schemes for the enzymatic syntheses of the green telechelics in $scCO_2$. An excess of diacid was used for alcohol end-cappers (SA, HEMA and TMPO), whilst an excess of diol was required in the case of the acid end-capper (HSA).

^1H and ^{13}C-NMR analysis. NMR analyses were conducted on a Bruker DPX300 spectrometer in $CDCl_3$ (20 mg/mL). The number of scans was 16 for ^1H (300 MHz) and 4096 for ^{13}C (75 MHz). Conversion and chains length were analysed through monomer peak and end-group analysis. The chemical shifts were reported in part per million (ppm) with respect to residual solvent peaks (7.26 ppm for ^1H and 77.36 ppm for ^{13}C) (58).

Gel permeation chromatography (GPC). The molecular weight distributions of the samples were analysed using a Polymer Laboratories GPC 50 with a refractive index detector and calibrated with poly(styrene) standards. The machine was equipped with a PL aquagel-OH 5 µm guard column followed by two PL aquagel-OH 20 5 µm columns. The samples were run in $CHCl_3$ Chromasolv® (5 mg/mL) at a flow rate of 1 mL/min. Cirrus software was used for analysis.

Differential scanning calorimetry (DSC). DSC analyses were performed using a TA-Q2000 DSC (TA Instruments, USA) calibrated with sapphire and indium standards. In a standard experiment, the sample (2.00 ± 0.10 mg) was melted with a first heating scan up to 100 °C (10 °C/min) and cooled down to -90 °C (10 °C/min). A second heating scan up to 100 °C, with the same heating rate, was then carried out to detect the melting point. Isothermal 5-minute segments were performed at the conclusion of each ramp. The experiments were carried out under a N_2 flow (50 mL/min).
The T_m was taken as the maximum of the endothermic peak. Each experiment was repeated three times and the results are shown as the average ± 1 standard deviation.

Matrix-assisted laser desorption/ionisation-Time of flight mass spectrometry (MALDI-TOF). MALDI-TOF analyses were performed using a Bruker UltraFlex III. DCTB (*i.e. trans*-2-[3-(4-*tert*-Butylphenyl)-2-methyl-2-propenylidene]malononitrile) was used as a matrix with Na^+ and K^+ as cations. The analyses were performed in reflection mode with laser intensity normally below 40%. For the sample preparation, 20 µL of a solution of polymer in $CHCl_3$ (10 mg/mL) were mixed with 20 µL of a DCTB solution in acetonitrile (10 mg/mL) and 0.5 µL of sodium and/or potassium trifluoroacetate in acetonitrile (5 mg/mL); 1 µL of this mixture was spotted on the target plate and left to dry at room temperature.

3. Results and discussion

3.1.1 Low temperature enzymatic route to telechelic PHA in $scCO_2$

Azelaic acid is a commercially available bio-based monomer, which has been exploited for polyester synthesis. In the current literature the polymerisations are typically performed by using metal catalysts at temperatures higher than 200 °C (56, 57). For the purpose of producing polymers with tailored functionalities, it is important to carry out selective polymerisation, hence a low temperature will be of great significance. This is particularly important for all those applications where thermally labile chemical groups (*e.g.* unsaturated ones) or bioactive molecules must be incorporated into the polymer.

Therefore, our approach is to use $scCO_2$ as the reaction medium for the production of a variety of telechelic polyesters based on azelaic acid, to demonstrate that it is possible to exploit a low temperature enzymatic route to synthesise functional polyazelates without pre-modification of the monomer and in a solvent-free system.

The reactions were carried out at 35 °C targeting the molecular weights by carefully controlling the monomer and end-capper feed ratios. Once the autoclave was vented, crystallised white products were collected. After separation of the enzyme/molecular sieves and drying, light yellow/white solid polymers were obtained (**Supplementary Material, Fig.1**).

All the reactions provided product in good yields and almost quantitative conversions (**Table 2**). Furthermore, enzyme-recycling tests showed that the lipase activity is not compromised during the high-pressure reactions and the commercially found enzyme can be re-used without loss of activity (**Supplementary Material, Fig. 2-3**).

Table 2 – Novozym 435-catalysed functional PHAs synthesis in $scCO_2$.

Product	M_n^{th} (g/mol)[a]	M_n^{NMR} (g/mol)[b]	M_n^{GPC} (g/mol)	$Đ$	T_m (°C)	ΔH_f (J/g)	Yield (%)[c]	Conversion (%)[d]
PHA-SA	1160	1500	2400	1.96	38.6 ± 0.9	65.5 ± 1.0	86	98
PHA-HSA	1493	1400	2400	1.83	46.0 ± 0.2	81.2 ± 3.5	88	99
PHA-TMPO	1196	1100	1500	1.73	29.1 ± 0.2	50.4 ± 0.8	87	96
PHA-HEMA	1230	1500	1700	2.18	31.0 ± 0.4	48.4 ± 0.5	78	98

[a]Calculated according to the reagents ratios; [b]Determined through ^{1}H-NMR from the ratio between the integrals of the peaks of the polymer backbone and the end-group peak; [c]Yield= weight of collected product/theoretical weight; [d]Determined through ^{1}H-NMR from the ratio of the 1,6-hexanediol peak at 3.65 ppm and the polyester peak at 4.10 ppm.

The conversion of each reaction was analysed by monitoring the peaks relative to 1,6-hexanediol in its pristine form (protons adjacent to the alcohol group) and when incorporated into the polymer backbone (protons adjacent to the ester group). All the reactions showed high conversion (≥96%) but it is worth pointing out that any polymers terminated with an alcohol group do also give a peak at 3.65 ppm and this does lead to a small underestimation of the conversion. MALDI-TOF data do show that there is a component of polymer that is alcohol terminated in PHA-TMPO (**Figure 9**).

3.1.2 Thermal properties

DSC analyses allowed for the determination of the thermal properties of the telechelics. The T_m and the enthalpy of fusion (ΔH_f) of the products can be seen to change significantly when varying the end-capper (**Figure 4**).

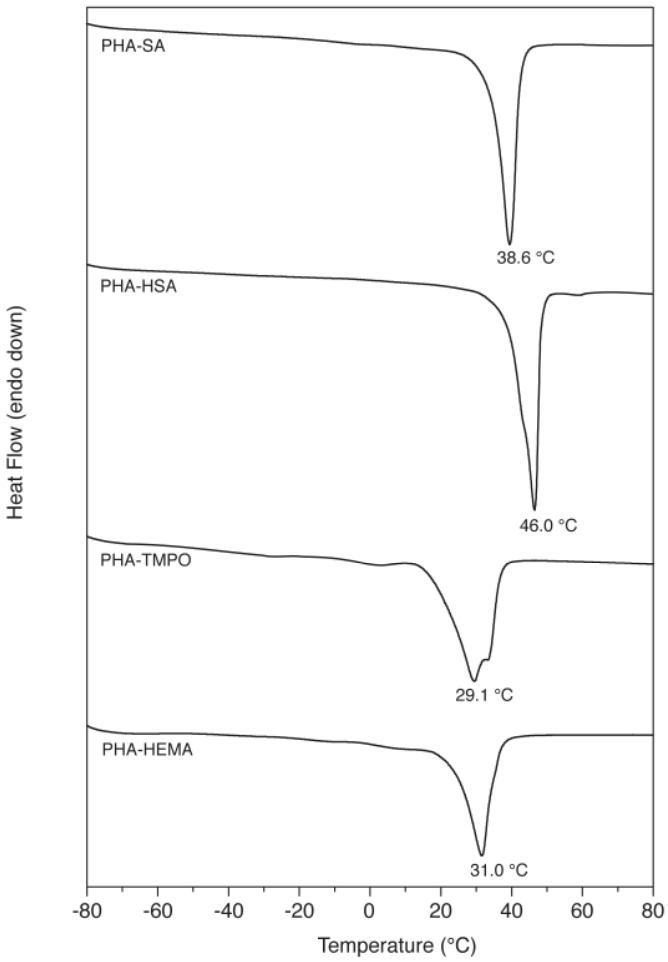

Figure 4 – DSC traces of PHA with different end-functionalisation. PHA-HSA displays the highest T_m (46.0 °C), whilst PHA-TMPO shows the lowest one (29.1 °C)

It is well known that the thermal properties of low molecular weight polymers can be strongly influenced by the end-groups (59, 60). Different end-groups can result in different crystallisation behaviours, therefore resulting in varied ΔH_f and T_m. (61). In more detail, the sharpest and largest endothermic peaks are shown by the HSA and SA functional PHAs, whilst PHA-TMPO and PHA-HEMA exhibit the lowest T_m and ΔH_f. This is due the bulkier structure of the latter end-cappers that alters more significantly the crystalline structure. A similar effect has been observed on phenoxyl and acetoxyl terminated low molecular weight (1000-3000 g/mol) poly(ethylene oxide) when compared to hydroxyl, methoxyl and ethoxyl terminated chains (62, 63).
In addition, PHA-TMPO exhibits a bimodal melting endotherm. It is well known that in semicrystalline polyesters multiple endothermic peaks, or multimodal melting points, can be detected. This arises from the melting of crystallites with different stability and size, or from crystals reorganisation (64). Therefore, this is the likely explanation for our observation with PHA-TMPO. Finally, it was not possible to clearly identify the T_g of the telechelics through DSC. This is common in highly crystalline systems. However, the T_g should be expected at around -60 °C as has been observed by others for similar polyesters, such as poly(butylene azelate) (64).

3.1.2 Structural characterisation

The M_n determined from ^{1}H-NMR is in all the cases close to the theoretical value calculated from the diacid : diols : functionaliser ratios. Thus, we demonstrate that the polymerisations yielded chains with DP within the desired range, suitable for coating applications and cross-linked networks (9, 10, 29). The M_n calculation was performed by use of the integral values assigned to the peaks of polymer backbone compared to those of end-group; thus assuming that all the polymer chains were di-functional. If this assumption was wrong the M_n values determined by ^{1}H-NMR would be vastly overestimated. To check this, GPC analyses were also used, and the results were found to be close to those calculated from ^{1}H-NMR (**Table 2**). However, there is clearly an overestimation in M_n^{GPC} for all the polymers, in particular for PHA-SA and PHA-HSA. This is a consequence of the calibration performed with poly(styrene) (PSt) standards, which will always have hydrodynamic volume different from the analysed

polyesters. Similar differences have been encountered by other groups, when using GPC with PSt standards for polyester analysis (9, 11, 65). Nevertheless, the dispersity values are mostly around 2, which is a value typically expected for linear polycondensations at high conversions and already found by other groups when synthesising low molecular weight telechelics (9, 15, 65, 66).
^{1}H-NMR (**Figure 5-1,2** and **Figure 6-1,2**) and ^{13}C-NMR (**Supplementary Material, Fig. 4-7**) analyses also confirm the chemical structure and incorporation of intact end-groups.

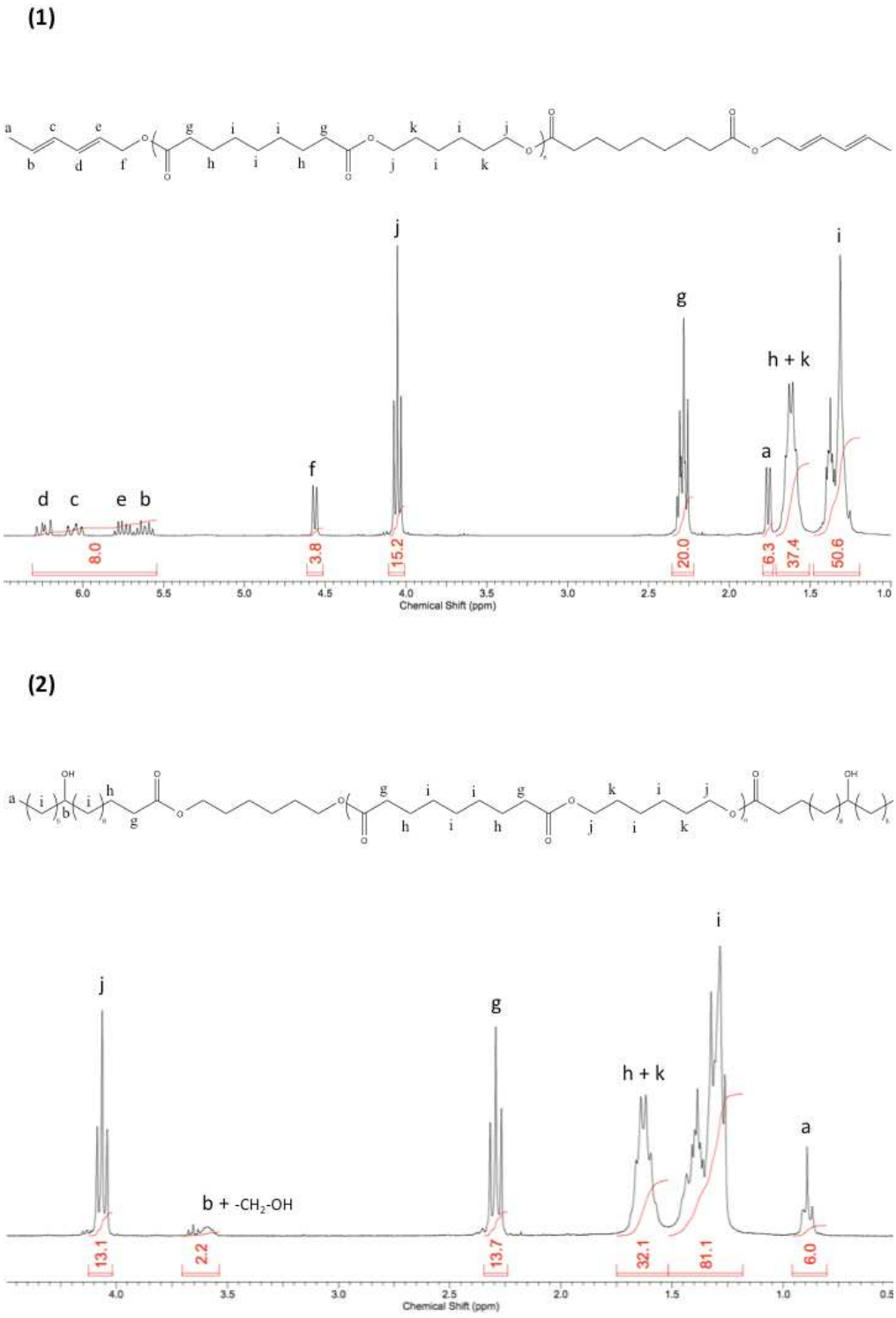

Figure 5 - ^{1}H-NMR of: (1) PHA-SA: the end-capper peaks are clearly observed at around 1.75 ppm (a), 4.52 ppm (f) and between 5.50 and 6.55 ppm (b-e); (2) PHA-HSA: the end-capper peaks are observed at 0.90 ppm (a), 3.60 ppm (b) and in the peak at 1.45 ppm (i). An additional small triplet that is assigned to protons adjacent to an alcohol group (either in the 1,6-hexanediol or uncapped chains) is observed at 3.65 ppm in PHA-HSA.

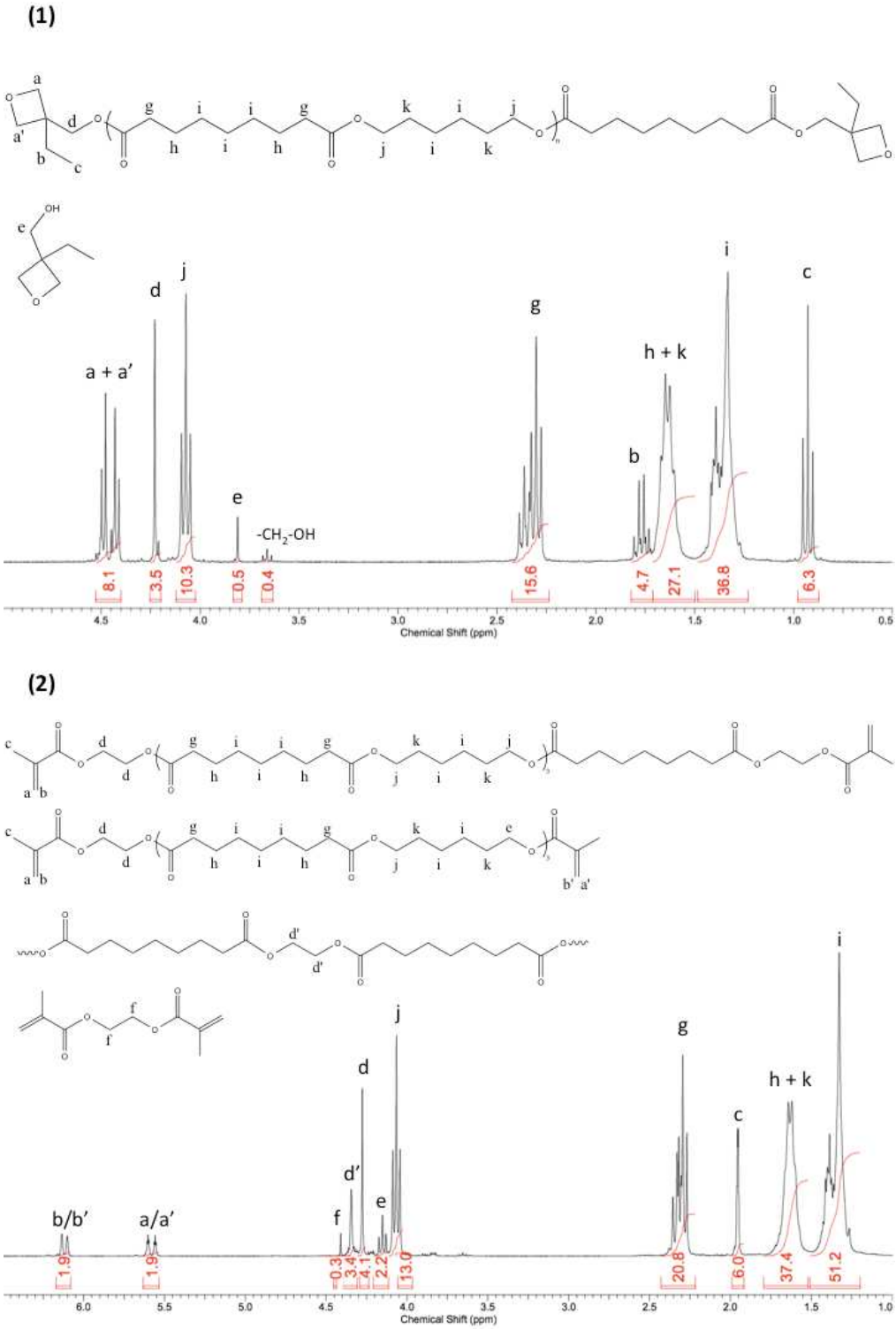

Figure 6 – ^{1}H-NMR of: (1) PHA-TMPO: the end-capper peaks are observed at around 4.50 ppm (a and a'), 1.75 ppm (b), 0.95 ppm (c) and 4.25 ppm (d), a peak assigned to unreacted TMPO (<13%) is observed at 3.81 ppm (e); (2) PHA-HEMA: the end-capper signals are seen at 5.55 ppm (a and a'), 6.65 ppm (b and b'), 1.98 ppm (c) and 4.28 (d). The peak d' is assigned to ethylene glycol incorporated in the backbone rather than at the end of the chains, and the peak f is given by the EGDMA (<4%) formed by the enzyme.

The ^{1}H-NMR spectra clearly show that the end-group functionalities are incorporated into the polymer chains and are unaffected during the synthesis mainly as a result to the low reaction temperature (35 °C) achieved by using $scCO_2$. It is well known that at higher temperatures (>85 °C) side reactions involving acrylate, methacrylate and oxetanes moieties do occur (27, 67). In addition, it is known that the selectivity of CaLB towards primary alcohol is significantly reduced at above 100 °C; thus leading to branching when monomers or end-capper with secondary -OH groups are exploited (65). Therefore, lower temperature approaches are highly desirable when using CaLB.

Furthermore, it is clear that in the spectrum of PHA-HEMA, in addition to the expected peaks, additional features can be assigned to different species (**Figure 6-2**). This likely occurs because CaLB interacts with the carbonyl group of HEMA, forming a tetrahedral intermediate followed by the formation of an acyl-enzyme complex. This step is then followed by the release of ethylene glycol that goes on to react with another acyl-enzyme complex formed with azelaic acid. Therefore, ethylene glycol units can be inserted in the telechelic backbone rather then at the end (**Figure 6-2**, peak *d'*). Equally, the acyl-enzyme complex with the methacrylate group can react with 1,6-hexanediol and, therefore, the methacrylate group will then be attached directly to it (**Figure 6-2**, peak *e*).
Finally, the same acyl-enzyme complex can react with HEMA forming the diester ethylene glycol dimethacrylate (EGDMA) (**Figure 6-2**, peak *f*), although less than 4% of this species is detected through ^{1}H-NMR.
This is a clear demonstration of the dynamic nature of lipase-catalysed reactions. CaLB is continuously cleaving ester linkages and creating new ones, thus causing the migration of ethylene glycol units throughout the polymer chains as shown in **Figure 6-2** and as reported in the literature (9).
Further verification of the end-group structures was obtained by MALDI-TOF analyses. These measurements confirmed successful enzymatic polymerisation and functionalisation. Several series of peaks with a repetitive pattern of 270.4 g/mol are detected for all the polymers, hence confirming the structure of the hexylene azelate repeating units.
In more detail, the spectrum of PHA-SA clearly show two main series that can be assigned to the di-functional polymer (n) (**Figure 7**). Only one peak with very low intensity assigned to a non-functional chain is detected, therefore confirming the ^{1}H-NMR results and a high extent of functionalisation.

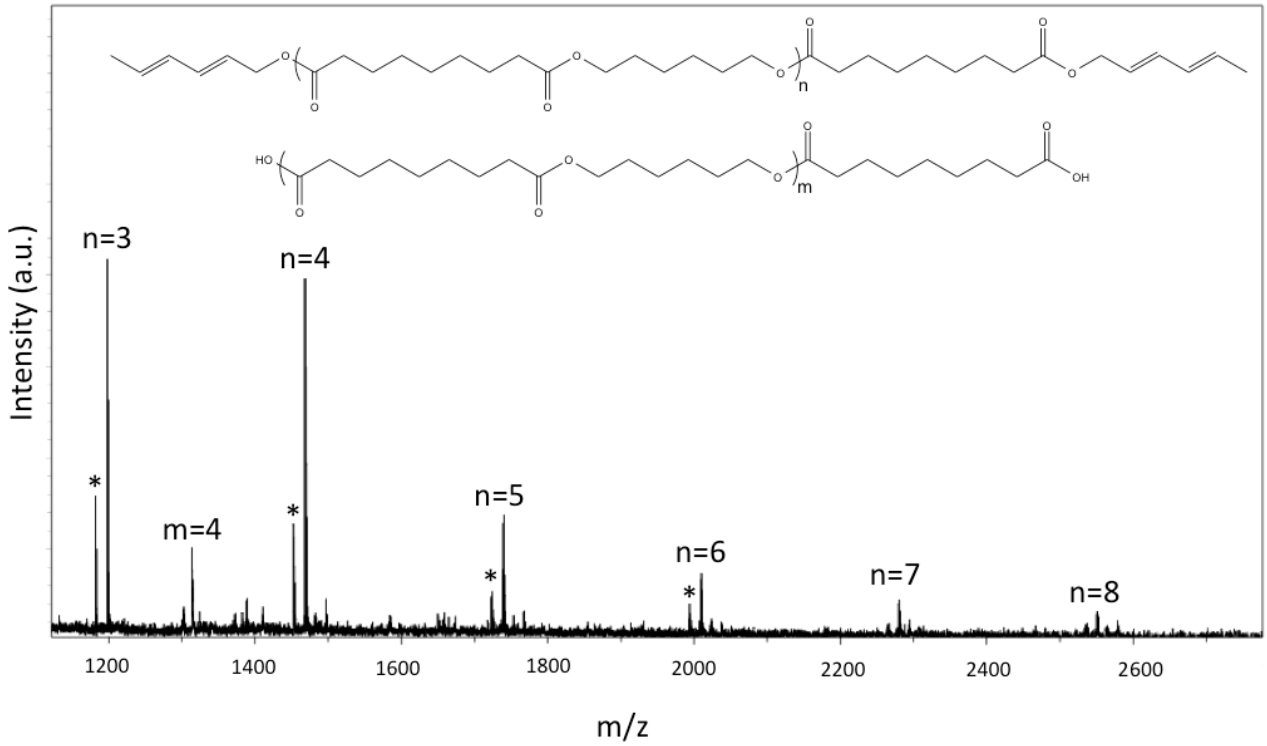

Figure 7 – MALDI-TOF spectrum of PHA-SA. The main series (n) is assigned to the telechelic chains ionised with K^+. Satellite signals at lower m/z (*) are given by chains with Na^+ ions. The peak m can be assigned to a non-functional (AB)A-type chain with DP4.

The spectrum of PHA-HSA shows only one series of peaks assigned to di-functional chains. No mono-functional or non-functional chains are detected (**Figure 8**).

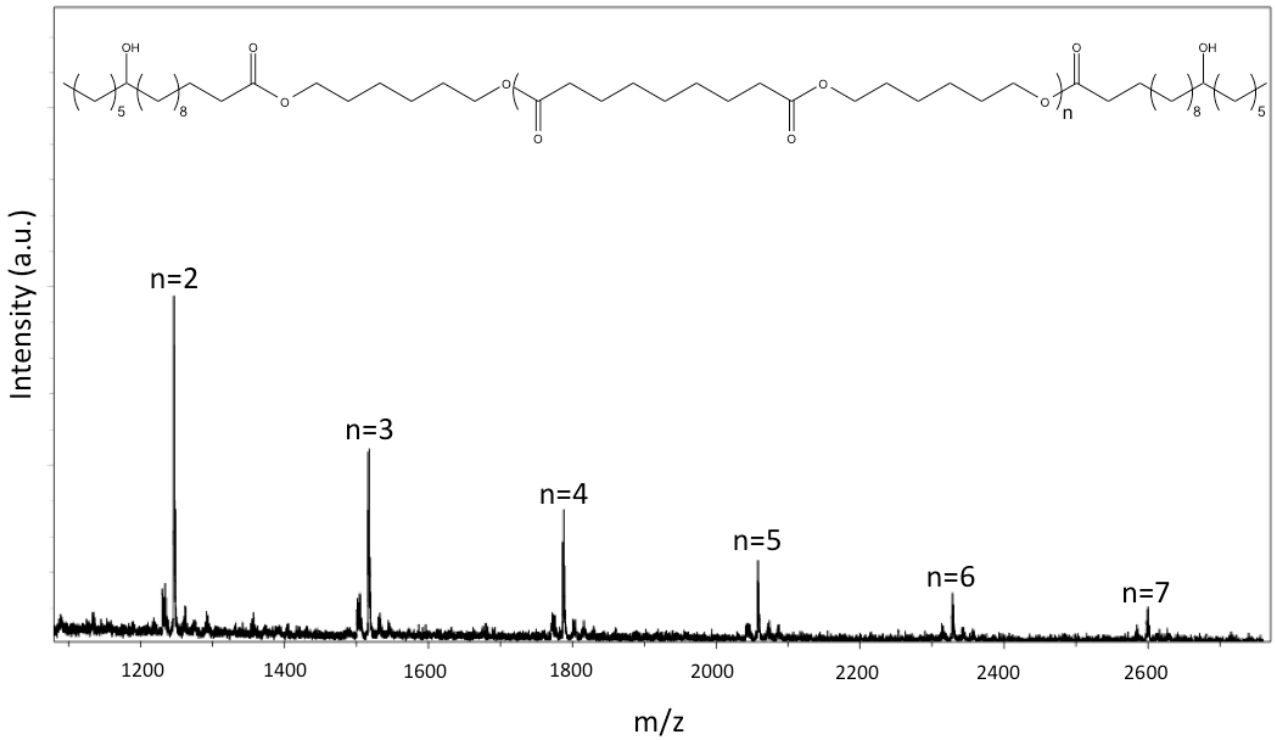

Figure 8 - MALDI-TOF spectrum of PHA-HSA. The main series (n) is given by the telechelic chains. No other species are detected.

By contrast, the MALDI-TOF spectrum of PHA-TMPO shows several different series (**Figure 9**). The main one (n) is given by the chains carrying oxetane moieties at both ends. In addition to this, two other distributions are detected. Both of them are assigned to non-functional AB-type polymer chains; one terminating with an alcohol and a free acid end (m), the other (*) with an alcohol and a sodium carboxylate end-group formed in the MALDI-TOF sample preparation. Sodium carboxylate end-groups have been already observed in the mass spectrum of similar systems (9).

Although the intensity of the AB-type polymer peaks is quite high, it should be noted that this analysis is not quantitative, thus the size of the peaks does not indicate absolute quantities but only how effectively different fragments are ionised and fly down the MALDI-TOF (11, 68). In fact, the non-functional AB-type chains represent around 18% of the product, as calculated from ^{1}H-NMR by analysis of the ratio between the peaks 4.20 ppm and at 3.65 ppm (**Figure 6-1**). Therefore, the targeted telechelic polyester represents more than 80% of the final product.

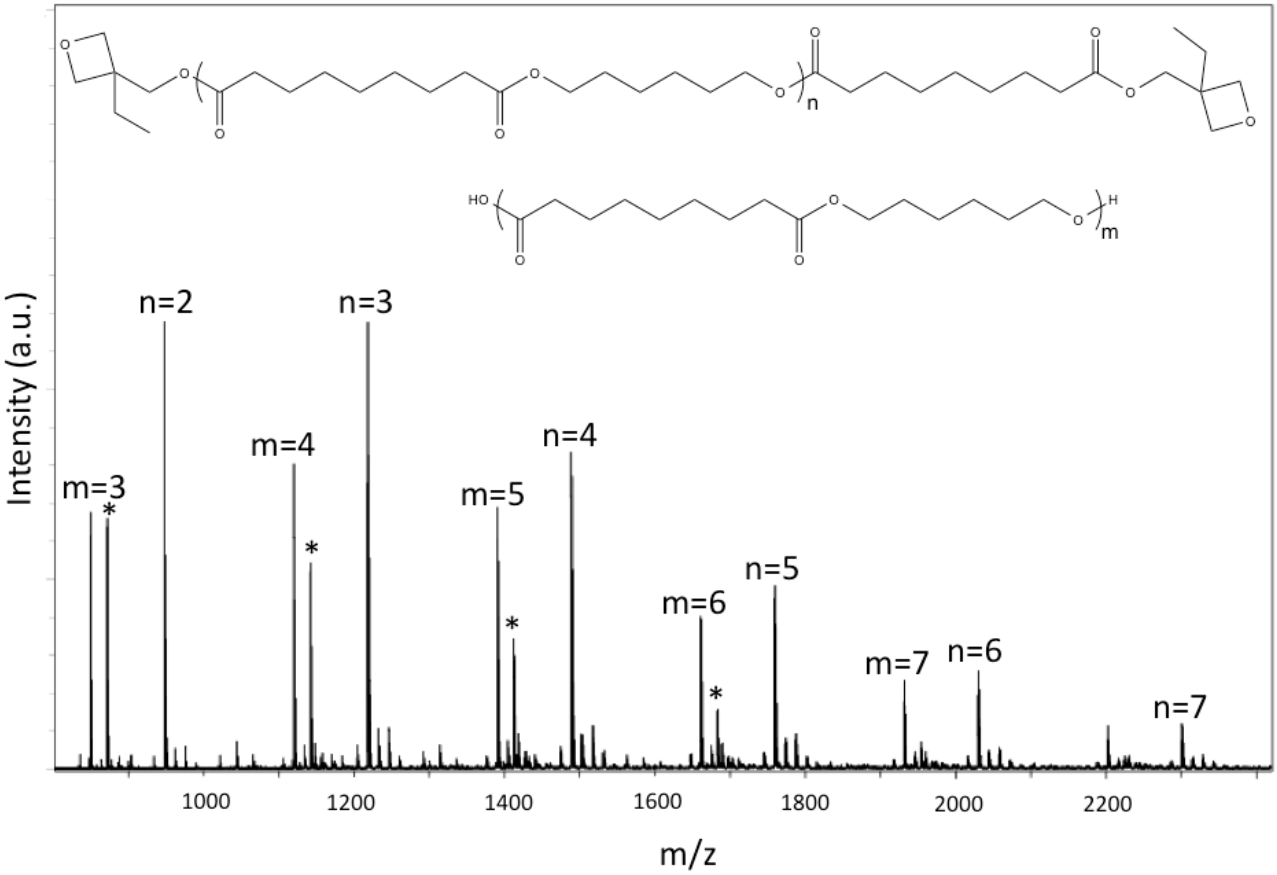

Figure 9 – MALDI-TOF spectrum of PHA-TMPO. (n) di-functional product; (m) AB-type chains with acid and alcohol end-group; (*) AB-type chains with a sodium carboxylate and an alcohol end.

Finally, the spectrum of PHA-HEMA shows once again the dynamic nature of lipase-catalysed polyesterifications (**Figure 10**). Five different species can be identified: three are di-functional and two mono-functional. These structures are differentiated by the presence or the absence of ethylene glycol units. Thus, confirming the ^{1}H-NMR results described previously (**Figure 6-2**). Nonetheless, non-functionalised structures were not detected, therefore all the polymer chains that are produced can participate in radical cross-linking reactions leading to useful functional materials.

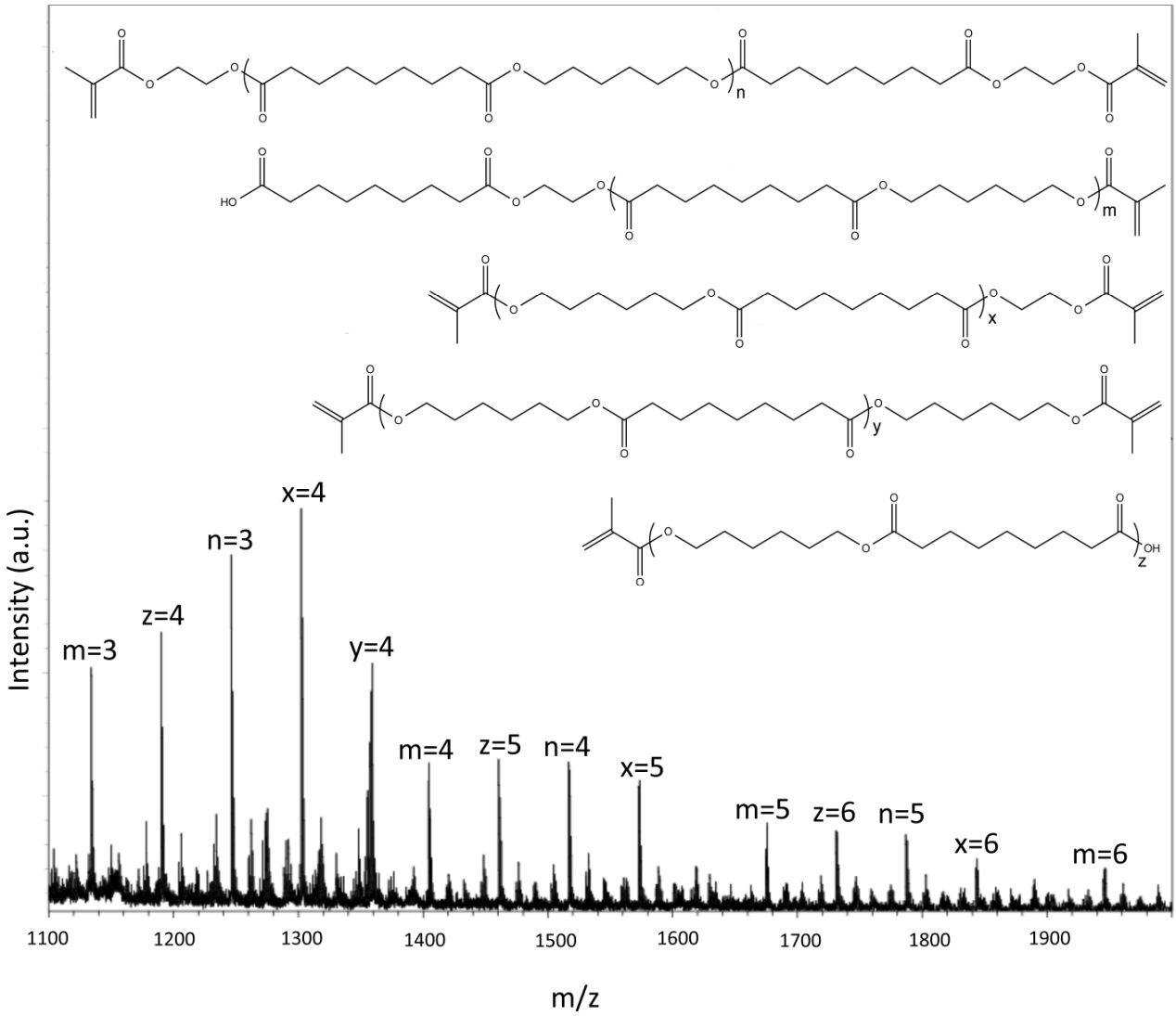

Figure 10 – MALDI-TOF spectrum of PHA-HEMA. Different species can be identified. (n), (x) and (y) are telechelic chains; (m) and (z) are mono-functional chains.

4. Conclusions

We demonstrate a low temperature approach using $scCO_2$ that allows us to exploit CaLB as a catalyst to synthesise four different telechelics by using azelaic acid and 1,6-hexanediol as building blocks of the backbone. This would have not been possible with conventional routes because of the high temperatures required to melt the monomer and activate metal catalysts. Furthermore, suitable solvents for the polycondensation are not available due to the insolubility of azelaic acid in apolar solvents. By use of CO_2 and the enzyme we achieved remarkably high yields and monomer conversion at low temperature (35 °C).

The chemical structures have been confirmed by ^{1}H-NMR and MALDI-TOF analyses, showing that all the products were successfully functionalised in a one pot-reaction.

The combined use of CaLB and $scCO_2$ (and consequent mild temperature) also avoid competing side reactions involving the end-group functionalities. Furthermore, enzyme-recycling tests demonstrate that the catalyst activity is not compromised during the high-pressure reactions and the immobilised lipase can be re-used without loss of activity.

The synthesised telechelics are valuable and could be exploited for further modification, cross-linking or chain extension processes. Therefore, we demonstrate by exploiting the unique properties of $scCO_2$ it is possible to synthesise useful renewable materials without the need for high temperatures, large amounts of conventional solvents or pre-modification of the monomers. This route could be especially valuable for applications involving the incorporation of thermally labile functional groups and/or molecules (*e.g.* proteins, drugs *etc.*).

Solvents, in small amount, were only used to separate the polymers from the enzyme beads. This could in principle be achieved by use of $scCO_2$ as a plasticiser, to effectively liquefy the polymer and accomplish the separation (25). This process will therefore lead towards a fully green, solvent-free, low-temperature route for the synthesis of

renewable functional polyesters in $scCO_2$. Such an approach would be of great importance in the production of functional materials for biomedical applications.

Additional Information

Acknowledgments
We are grateful to Novozymes (Denmark) for the kind gift of Novozyme 435. We thank Richard Wilson, Pete Fields and Mark Guyler (University of Nottingham) for the technical input with the high-pressure equipment.
Prof S.M. Howdle is delighted to acknowledge Sir Martyn Poliakoff FRS and in particular to thank him for his guidance, encouragement and fatherly advice.

Funding Statement
The research leading to these results (SC) has received funding from the People Programme (Marie Curie Actions) of the European Union's Seventh Framework Programme FP7/2007-2013/ under REA grants agreement No. [289253].

Data Accessibility
Additional data supporting this article have been uploaded as part of the Supplementary Material. They are available online or from the author.

Authors' Contributions
The PhD student S. Curia carried out most of the experiments and characterisation, interpreting the results and writing the manuscript. Undergraduate student A.F. Barclay contributed to the experimental data and characterisation studies. Prof M. Johansson and the PhD student S. Torron advised on end-group modification and characterisation. Prof S.M. Howdle conceived and designed the experiments with S. Curia.

Acronyms

CaLB	→	Candida antarctica Lipase B
DCTB	→	trans-2-[3-(4-tert-Butylphenyl)-2-methyl-2-propenylidene]malononitrile
DP	→	Degree of polymerisation
DSC	→	Differential scanning calorimetry
EGDMA →	Ethylene glycol dimethacrylate	
HEMA	→	2-hydroxyethyl methacrylate
HSA	→	12-hydroxy stearic acid
PHA	→	Poly(hexylene azelate)
RT	→	Room temperature
SA	→	Sorbic alcohol
$scCO_2$	→	Supercritical CO_2
SFC	→	Supercritical fluid chromatography
TMPO	→	Trimethylolpropane oxetane

References

1. Cordeiro N, Belgacem NM, Gandini A, Pascoal Neto C. Cork Suberin as a New Source of Chemicals: 2. Crystallinity, Thermal and Rheological Properties. Bioresource Technology. 1998;63:153-5.
2. Gandini A, Pascoal Neto C, Silvestre AJD. Suberin: A promising renewable resource for novel macromolecular materials. Progress in Polymer Science. 2006;31(10):878-92.
3. Gandini A. Polymers from Renewable Resources A Challenge for the Future of Macromolecular Materials. Macromolecules. 2008;41(24):9491-504.
4. Belgacem MN, Gandini A. Monomers, Polymers and Composites from Renewable Resources: Elsevier Science; 2011.
5. Curlee TR, Das S, Agency USEP. Plastic Wastes: Management, Control, Recycling, and Disposal: Noyes Data Corporation; 1991.
6. Siracusa V, Rocculi P, Romani S, Rosa MD. Biodegradable polymers for food packaging: a review. Trends in Food Science & Technology. 2008;19(12):634-43.
7. Ulery BD, Nair LS, Laurencin CT. Biomedical Applications of Biodegradable Polymers. Journal of polymer science Part B, Polymer physics. 2011;49(12):832-64.
8. Eriksson M, Fogelström L, Hult K, Malmström E, Johansson M, Trey S, et al. Enzymatic One-Pot Route to Telechelic Polypentadecalactone Epoxide: Synthesis, UV Curing, and Characterization. Biomacromolecules. 2009;10(11):3108-13.
9. Eriksson M, Hult K, Malmström E, Johansson M, Trey SM, Martinelle M. One-pot enzymatic polycondensation to telechelic methacrylate-functional oligoesters used for film formation. Polymer Chemistry. 2011;2(3):714-9.
10. Torron S, Semlitsch S, Martinelle M, Johansson M. Polymer Thermosets from Multifunctional Polyester Resins Based on Renewable Monomers. Macromolecular Chemistry and Physics. 2014;215(22):2198-206.
11. Rüdiger A, Hendil-Forssell P, Hedfors C, Martinelle M, Trey S, Johansson M. Chemoenzymatic Route to Renewable Thermosets Based on a Suberin Monomer. Journal of Renewable Materials. 2013;1(2):16.
12. McNaught AD, Wilkinson A. IUPAC. Compendium of Chemical Terminology, 2nd ed. (the "Gold Book). Oxford: Blackwell Scientific Publications; 1997.
13. Ren J, Hua X, Zhang T, Zhang Z, Ji Z, Gu N. Grafting of telechelic poly(lactic-co-glycolic acid) onto O2 plasma-treated polypropylene flakes. Journal of Applied Polymer Science. 2011;121(1):210-6.
14. Keul H, Neumann A, Reining B, Höcker H. Synthesis of telechelics and block copolymers via “living” radical polymerization. Macromolecular Symposia. 2000;161(1):63-72.
15. Simpson N, Takwa M, Hult K, Johansson M, Martinelle M, Malmström E. Thiol-Functionalized Poly(ω-pentadecalactone) Telechelics for Semicrystalline Polymer Networks. Macromolecules. 2008;41(10):3613-9.
16. Roe FJC, Boyland E, Millican K. Effects of oral administration of two tin compounds to rats over prolonged periods. Food and Cosmetics Toxicology. 1965;3:277-80.
17. de Groot AP, Feron VJ, Til HP. Short-term toxicity studies on some salts and oxides of tin in rats. Food and Cosmetics Toxicology. 1973;11(1):19-30.
18. Howe P, Watts P. Tin and Inorganic Tin Compounds. Geneva: World Health Organization, 2005.
19. Zhang J, Shi H, Wu D, Xing Z, Zhang A, Yang Y, et al. Recent developments in lipase-catalyzed synthesis of polymeric materials. Process Biochemistry. 2014;49(5):797-806.
20. Dubois P, Coulembier O, Raquez JM. Handbook of Ring-Opening Polymerization: Wiley; 2009.
21. Montaudo G, Rizzarelli P. Synthesis and enzymatic degradation of aliphatic copolyesters. Polymer Degradation and Stability. 2000 //;70(2):305-14.
22. Bikiaris DN, Papageorgiou GZ, Achilias DS. Synthesis and comparative biodegradability studies of three poly(alkylene succinate)s. Polymer Degradation and Stability. 2006;91(1):31-43.
23. Papageorgiou GZ, Bikiaris DN. Synthesis, Cocrystallization, and Enzymatic Degradation of Novel Poly(butylene-co-propylene succinate) Copolymers. Biomacromolecules. 2007 2007/08/01;8(8):2437-49.
24. Papageorgiou GZ, Bikiaris DN, Achilias DS, Nanaki S, Karagiannidis N. Synthesis and comparative study of biodegradable poly(alkylene sebacate)s. Journal of Polymer Science Part B: Polymer Physics. 2010;48(6):672-86.
25. Loeker FC, Duxbury CJ, Kumar R, Gao W, Gross RA, Howdle SM. Enzyme-Catalyzed Ring-Opening Polymerization of epsilon-Caprolactone in Supercritical Carbon Dioxide. Macromolecules. 2004;37:2450-3.
26. Olsson A, Lindström M, Iversen T. Lipase-Catalyzed Synthesis of an Epoxy-Functionalized Polyester from the Suberin Monomer cis-9,10-Epoxy-18-hydroxyoctadecanoic Acid. Biomacromolecules. 2007;8:757-60.
27. Zhan F, Asif A, Liu J, Wang H, Shi W. Synthesis and properties of cationic photopolymerizable hyperbranched polyesters with terminal oxetane groups by the couple-monomer polymerization of carboxylic anhydride with hydroxyl oxetane. Polymer. 2010;51(15):3402-9.
28. Poojari Y, Clarson SJ. Thermal stability of Candida antarctica lipase B immobilized on macroporous acrylic resin particles in organic media. Biocatalysis and Agricultural Biotechnology. 2013;2(1):7-11.

29. Torron S, Johansson M. Oxetane-terminated telechelic epoxy-functional polyesters as cationically polymerizable thermoset resins: Tuning the reactivity with structural design. Journal of Polymer Science Part A: Polymer Chemistry. 2015;53(19):2258-66.
30. Japu C, Martinez de Ilarduya A, Alla A, Jiang Y, Loos K, Munoz-Guerra S. Copolyesters Made from 1,4-Butanediol, Sebacic Acid, and d-Glucose by Melt and Enzymatic Polycondensation. Biomacromolecules. 2015;16(3):868-79.
31. Jiang Y, Woortman AJ, van Ekenstein GO, Loos K. Enzyme-catalyzed synthesis of unsaturated aliphatic polyesters based on green monomers from renewable resources. Biomolecules. 2013;3(3):461-80.
32. Tsioptsias C, Paraskevopoulos MK, Christofilos D, Andrieux P, Panayiotou C. Polymeric hydrogels and supercritical fluids: The mechanism of hydrogel foaming. Polymer. 2011;52(13):2819-38.
33. Gutiérrez C, Garcia MT, Curia S, Howdle SM, Rodriguez JF. The effect of CO2 on the viscosity of polystyrene/limonene solutions. The Journal of Supercritical Fluids. 2014;88:26-37.
34. Picchioni F. Supercritical carbon dioxide and polymers: an interplay of science and technology. Polymer International. 2014;63(8):1364-99.
35. Jennings J, Beija M, Kennon JT, Willcock H, O'Reilly RK, Rimmer S, et al. Advantages of Block Copolymer Synthesis by RAFT-Controlled Dispersion Polymerization in Supercritical Carbon Dioxide. Macromolecules. 2013;46(17):6843-51.
36. Du L, Kelly JY, Roberts GW, DeSimone JM. Fluoropolymer synthesis in supercritical carbon dioxide. The Journal of Supercritical Fluids. 2009;47(3):447-57.
37. Jennings J, Beija M, Richez AP, Cooper SD, Mignot PE, Thurecht KJ, et al. One-pot synthesis of block copolymers in supercritical carbon dioxide: a simple versatile route to nanostructured microparticles. Journal of the American Chemical Society. 2012;134(10):4772-81.
38. Tsivintzelis I, Pavlidou E, Panayiotou C. Biodegradable polymer foams prepared with supercritical CO2–ethanol mixtures as blowing agents. The Journal of Supercritical Fluids. 2007;42(2):265-72.
39. Bungert B, Sadowski G, Arlt W. Supercritical antisolvent fractionation: measurements in the systems monodisperse and bidisperse polystyrenecyclohexanecarbon dioxide. Fluid Phase Equilibria. 1997;139:349-59.
40. Nalawade SP, Picchioni F, Janssen LPBM. Batch production of micron size particles from poly(ethylene glycol) using supercritical CO2 as a processing solvent. Chemical Engineering Science. 2007;62(6):1712-20.
41. Kelly CA, Naylor A, Illum L, Shakesheff KM, Howdle SM. Supercritical CO2: A Clean and Low Temperature Approach to Blending PDLLA and PEG. Advanced Functional Materials. 2012;22(8):1684-91.
42. Howdle SM, Watson MS, Whitaker MJ, Davies MC, Shakesheff KM, Popov VK, et al. Supercritical fluid mixing: preparation of thermally sensitive polymer composites containing bioactive materials. Chemical Communications. 2001 (1):109-10.
43. Zhang Z, Handa YP. CO2-Assisted Melting of Semicrystalline Polymers. Macromolecules. 1997;30(26):8505-7.
44. Gourgouillon D, Avelino HMNT, Fareleira JMNA, Nunes da Ponte M. Simultaneous viscosity and density measurement of supercritical CO2-saturated PEG 400. The Journal of Supercritical Fluids. 1998;13(1–3):177-85.
45. Alessi P, Cortesi A, Kikic I, Vecchione F. Plasticization of Polymers with Supercritical Carbon Dioxide: Experimental Determination of Glass-Transition Temperatures. Journal of Applied Polymer Science. 2002;88:2189-93.
46. Boyer SAE, Grolier JPE. Modification of the glass transitions of polymers by high-pressure gas solubility. Pure and Applied Chemistry. 2005;77(3):593-603.
47. Lee M, Tzoganakis C, Park CB. Extrusion of PE/PS blends with supercritical carbon dioxide. Polymer Engineering & Science. 1998;38(7):1112-20.
48. Zhang Z, Handa YP. An in-situ study of plasticization of polymers by high-pressure gases. Journal of Polymer Science Part B: Polymer Physics. 1998;36(6):977-83.
49. Joseph R. Royer JMDS, Saad A. Khan. High-Pressure Rheology and Viscoelastic Scaling Predictions of Polymer Melts Containing Liquid and Supercritical Carbon Dioxide. Journal of Polymer Science Part B: Polymer Physics. 2001;39:3055-66.
50. Pini R, Storti G, Mazzotti M, Tai H, Shakesheff KM, Howdle SM. Sorption and swelling of poly(DL-lactic acid) and poly(lactic-co-glycolic acid) in supercritical CO2: An experimental and modeling study. Journal of Polymer Science Part B: Polymer Physics. 2008;46(5):483-96.
51. Yu L, Liu H, Chen L. Thermal behaviors of polystyrene plasticized with compressed carbon dioxide in a sealed system. Polymer Engineering & Science. 2009;49(9):1800-5.
52. Curia S, De Focatiis DSA, Howdle SM. High-pressure rheological analysis of CO2-induced melting point depression and viscosity reduction of poly(ε-caprolactone). Polymer. 2015;69:17-24.
53. Sparks DL, Hernandez R, Estévez LA, Meyer N, French T. Solubility of Azelaic Acid in Supercritical Carbon Dioxide. Journal of Chemical & Engineering Data. 2007;52:1246-9.
54. Sun Yu J, Keun Kim A. Effect of combination of taurine and azelaic acid on antimelanogenesis in murine melanoma cells. J Biomed Sci. 2010;17:1-5.
55. Arpe HJ. Ullmann's Encyclopedia of Industrial Chemistry, Ullmann's Encyclopedia of Industrial Chemistry: Set: Printed Fifth Edition plus Sixth Edition Electronic Release: Wiley; 1999.
56. Papageorgiou GZ, Bikiaris DN, Achilias DS, Karagiannidis N. Synthesis, Crystallization, and Enzymatic Degradation of the Biodegradable Polyester Poly(ethylene azelate). Macromolecular Chemistry and Physics. 2010;211(24):2585-95.

57. Papageorgiou GZ, Bikiaris DN, Achilias DS, Papastergiadis E, Docoslis A. Crystallization and biodegradation of poly(butylene azelate): Comparison with poly(ethylene azelate) and poly(propylene azelate). Thermochimica Acta. 2011;515:13-23.
58. Gottlieb HE, Kotlyar V, Nudelman A. NMR Chemical Shifts of Common Laboratory Solvents as Trace Impurities. The Journal of Organic Chemistry. 1997;62(21):7512.
59. Yamada T, Imamura Y. Relation between characteristics and melting point of oligomers in poly(ethylene terephthalate) manufacturing. Polymer Engineering & Science. 1988;28(6):381-4.
60. Lai W-C, Liau W-B, Lin T-T. The effect of end groups of PEG on the crystallization behaviors of binary crystalline polymer blends PEG/PLLA. Polymer. 2004;45(9):3073-80.
61. Mandelkern L. Crystallization of Polymers: Volume 1, Equilibrium Concepts: Cambridge University Press; 2002.
62. Ashman PC, Booth C. Melting of low molecular weight poly(ethylene oxide) with acetoxy- and trimethylsiloxy-end-groups. Polymer. 1973;14(7):300-2.
63. Fraser MJ, Cooper DR, Booth C. Crystallinity and fusion of low molecular weight poly(ethylene oxide): effect of end-group. Polymer. 1977;18(8):852-4.
64. Kong X, Qi H, Curtis JM. Synthesis and characterization of high-molecular weight aliphatic polyesters from monomers derived from renewable resources. Journal of Applied Polymer Science. 2014;131(15):1-9.
65. Gustini L, Noordover BAJ, Gehrels C, Dietz C, Koning CE. Enzymatic synthesis and preliminary evaluation as coating of sorbitol-based, hydroxy-functional polyesters with controlled molecular weights. European Polymer Journal. 2015;67:459-75.
66. Yokozawa T, Yokoyama A. Chain-Growth Polycondensation: Living Polymerization Nature in Polycondensation and Approach to Condensation Polymer Architecture. Polym J. 2004 02//print;36(2):65-83.
67. Schuchardt JL, inventor; Arco Chemical Technology, Inc., assignee. Preparation of oxetane polyether polyols using a bleaching earth catalyst. US patent US4970295 A
. 1990.
68. Li L. MALDI Mass Spectrometry for Synthetic Polymer Analysis: Wiley; 2009.

Tables

Table 1

Name	Functionaliser
PHA-SA	Sorbic alcohol (SA)
PHA-HSA	12-hydroxy stearic acid (HSA)
PHA-TMPO	Trimethylolpropane oxetane (TMPO)
PHA-HEMA	2-hydroxyethyl methacrylate (HEMA)

Table 2

Product	M_n^{th} (g/mol)[a]	M_n^{NMR} (g/mol)[b]	M_n^{GPC} (g/mol)	$Đ$	T_m (°C)	ΔH_f (J/g)	Yield (%)[c]	Conversion (%)[d]
PHA-SA	1160	1500	2400	1.96	38.6 ± 0.9	65.5 ± 1.0	86	98
PHA-HSA	1493	1400	2400	1.83	46.0 ± 0.2	81.2 ± 3.5	88	99
PHA-TMPO	1196	1100	1500	1.73	29.1 ± 0.2	50.4 ± 0.8	87	96
PHA-HEMA	1230	1500	1700	2.18	31.0 ± 0.4	48.4 ± 0.5	78	98

[a]Calculated according to the reagents ratios; [b]Determined through ^{1}H-NMR from the ratio between the integrals of the peaks of the polymer backbone and the end-group peak; [c]Yield= weight of collected product/theoretical weight; [d]Determined through ^{1}H-NMR from the ratio of the 1,6-hexanediol peak at 3.65 ppm and the polyester peak at 4.10 ppm.

Figure and table captions

Figure 1 – Azelaic acid is a naturally occurring diacid with T_m ~110 °C. 2
Figure 2 - The functional end-cappers used in this study. 2
Figure 3 – Reaction schemes for the enzymatic syntheses of the green telechelics in $scCO_2$. An excess of diacid was used for alcohol end-cappers (SA, HEMA and TMPO), whilst an excess of diol was required in the case of the acid end-capper (HSA). 4
Figure 4 – DSC traces of PHA with different end-functionalisation. PHA-HSA displays the highest T_m (46.0 °C), whilst PHA-TMPO shows the lowest one (29.1 °C) 6
Figure 5 - ^{1}H-NMR of: (1) PHA-SA: the end-capper peaks are clearly observed at around 1.75 ppm (a), 4.52 ppm (f) and between 5.50 and 6.55 ppm (b-e); (2) PHA-HSA: the end-capper peaks are observed at 0.90 ppm (a), 3.60 ppm (b) and in the peak at 1.45 ppm (i). An additional small triplet that is assigned to protons adjacent to an alcohol group (either in the 1,6-hexanediol or uncapped chains) is observed at 3.65 ppm in PHA-HSA. 7
Figure 6 – ^{1}H-NMR of: (1) PHA-TMPO: the end-capper peaks are observed at around 4.50 ppm (a and a'), 1.75 ppm (b), 0.95 ppm (c) and 4.25 ppm (d), a peak assigned to unreacted TMPO (<13%) is observed at 3.81 ppm (e); (2) PHA-HEMA: the end-capper signals are seen at 5.55 ppm (a and a'), 6.65 ppm (b and b'), 1.98 ppm (c) and 4.28 (d). The peak d' is assigned to ethylene glycol incorporated in the backbone rather than at the end of the chains, and the peak f is given by the EGDMA (<4%) formed by the enzyme. 8
Figure 7 – MALDI-TOF spectrum of PHA-SA. The main series (n) is assigned to the telechelic chains ionised with K^+. Satellite signals at lower m/z (*) are given by chains with Na^+ ions. The peak m can be assigned to a non-functional (AB)A-type chain with DP4. 9
Figure 8 - MALDI-TOF spectrum of PHA-HSA. The main series (n) is given by the telechelic chains. No other species are detected. 10
Figure 9 – MALDI-TOF spectrum of PHA-TMPO. (n) di-functional product; (m) AB-type chains with acid and alcohol end-group; (*) AB-type chains with a sodium carboxylate and an alcohol end. 11
Figure 10 – MALDI-TOF spectrum of PHA-HEMA. Different species can be identified. (n), (x) and (y) are telechelic chains; (m) and (z) are mono-functional chains. 12

Table 1 – Naming scheme of the telechelic poly(hexylene azelate)s (PHAs) presented in this paper 3
Table 2 – Novozym 435-catalysed functional PHAs synthesis in $scCO_2$. 5